

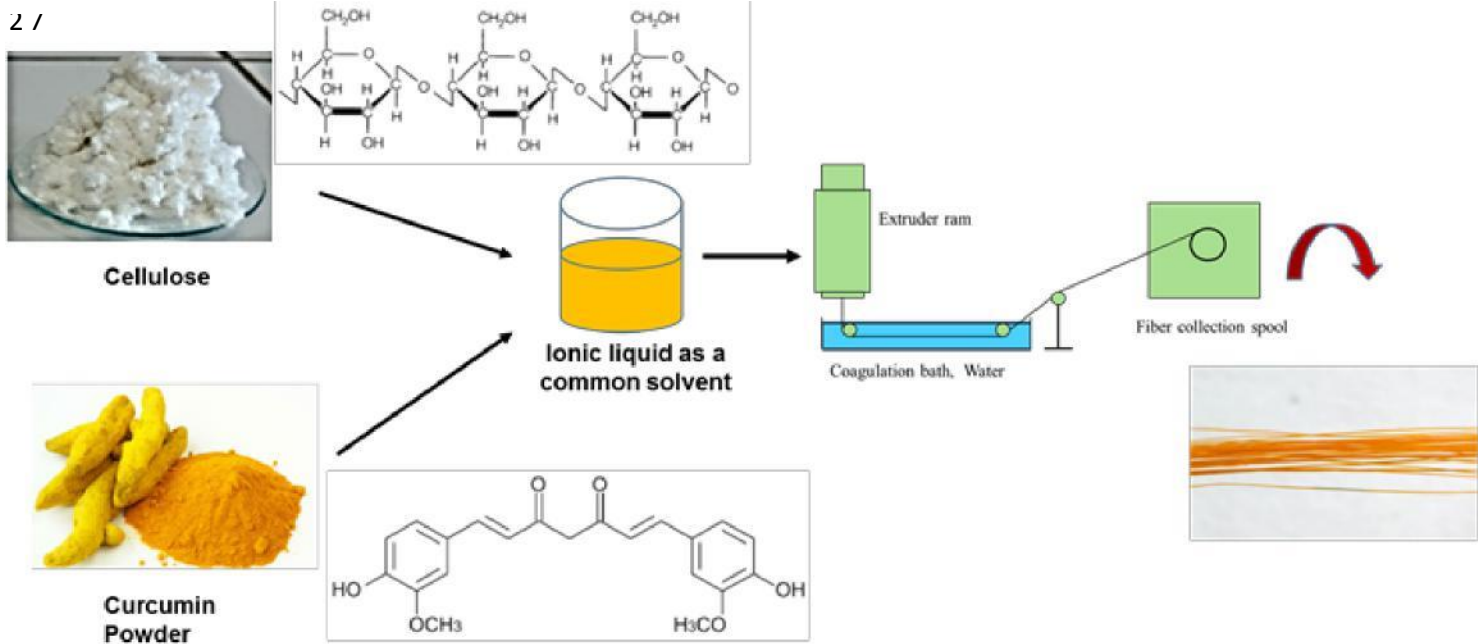
23

24

25

26

Graphical Abstract



Graphic Abstract

28 **Highlights**

29 1. Curcumin/cellulose composite fibres were manufactured using wet spinning
30 method.

31 2. The fibres showed high degree of alignment and good mechanical properties.

32 3. The fibres can be woven for use in bio-medical and food industry.

33 **Abstract**

34 We report a novel manufacturing method for bio renewable regenerated
35 cellulose fibres modified with curcumin, a molecule is known for its medicinal
36 properties. Ionic liquid namely 1-Ethyl 3-Methyl Imidazolium diethyl
37 phosphate (emim DEP) was found to be capable of dissolving cellulose as well
38 as curcumin. Regenerated cellulose/curcumin composites fibres with curcumin
39 concentration ranging from 1 to 10wt% were manufactured using dry jet wet
40 fibres spinning process using three different winding speeds. All the cellulose
41 and curcumin composite fibres showed distinct yellow colour imparted by
42 curcumin. The resultant fibres were characterised using scanning electron
43 microscopy (SEM), infrared spectroscopy, mechanical testing, and X-Ray
44 diffraction studies. Scanning electron microscopy of cellulose/curcumin fibres
45 cross-section did not show curcumin aggregates in cellulose fibres indicating
46 uniform dispersion of curcumin in cellulose matrix. The cellulose chain
47 alignment in cellulose/curcumin composite fibres resulted in tensile strength
48 ranging from 223 to 336 MPa and Young's modulus ranging from 13 to 14.9
49 GPa. The mechanical properties of cellulose/curcumin composite fibres thus

50 obtained are better than some of the commercially available regenerated
51 cellulose viscose fibres. The wide-angle X-ray diffraction analysis of
52 cellulose/curcumin composite fibres showed good alignment of cellulose chains
53 along the fibre axis. Thus, our findings are a major step in manufacturing strong
54 cellulose fibres with a pharmacologically potent drug curcumin which in future
55 could be used for medicinal, cosmetic and food packaging applications.

56

57 **Keywords:** Curcumin, cellulose, ionic liquids, fibres, textiles, food packaging.

58

59 1. Introduction

60 Among different bio renewable materials, cellulose is one of the most
61 common natural polymers found in higher plants, algae, bacteria, fungi and
62 marine animals. It is a linear polymer that consists of two glucose sugar units
63 that are linked by β -1, 4 glycosidic linkage to form a dimer known as
64 cellobiose (Eichhorn et al., 2010; Kontturi et al., 2006). The length of
65 cellulose chains can be very different due to the number of repeating units of
66 glucose (from 20 to 10 000 or more), also called degree of polymerization
67 or DP (Sidhu et al., 1998). Several studies have shown that cellulose and its
68 derivatives have a good biocompatibility and in addition, can be regarded as
69 slowly degradable materials (Czaja et al., 2007; Granja et al., 2005; Martson
70 et al., 1999; Miyamoto et al., 1989; Müller et al., 2006). Due to its excellent
71 mechanical and barrier properties, biocompatibility and low cost, cellulose is

72 used in many biomedical applications, like orthopedic devices and tissue
73 engineering (Granja et al., 2001; Poustis et al., 1994; Svensson et al., 2005)
74 and is an excellent candidate for food packaging (de Moura et al., 2012;
75 Imran et al., 2010). Several studies have indicated that some herbal
76 supplements contain phytochemicals that are able to prevent various relevant
77 and wide-spread pathologies, including diabetes, cancer and autoimmune
78 diseases (Aggarwal et al., 2008; Kaefer and Milner, 2008; Mahmood et al.,
79 2015). Among these many studies have reported that curcumin, a
80 polyphenol derived from *Curcuma longa*, commonly called turmeric, has
81 excellent pharmacological properties like antimicrobial, antiviral, anti-
82 inflammatory and anti-tumor activities (Ramsewak et al., 2000; Ruby et al.,
83 1995). Previous studies on wound healing in diabetic rats as well as
84 genetically diabetic mice have shown the efficacy of curcumin treatment
85 both by the oral and topical application. There was an improved
86 neovascularization, earlier re-epithelialization, increased migration of
87 various cells including fibroblasts, and dermal myofibroblasts, when
88 curcumin was used to treat the wounds of animals. (Sidhu et al., 1999; Sidhu
89 et al., 1998). Furthermore, curcumin has been widely used as an active
90 component in the food industry to create new packaging films with
91 antioxidant and antimicrobial activities (Sonkaew et al., 2012; Vimala et al.,
92 2011).

93 Ionic liquids (ILs) are a new class of benign solvents that can be liquid at
94 room temperature (usually $T_{\text{melt}} < 100\text{ }^{\circ}\text{C}$) (Holbrey and Rogers, 2002). Over
95 the past 20 years many studies have shown the countless properties of ionic
96 liquids, in particular their low volatility that makes them benign solvents as
97 compared to traditional volatile and aggressive solvents used for dissolving
98 cellulose (Carbon disulphide, sulfuric acid etc). ILs have good chemical and
99 thermal stability, high ionic and thermal conductivity, high heat capacity and
100 easy recyclability. All these properties can reduce many health and
101 environmental related issues when ILs are used as solvents for the
102 dissolutions of natural polymers like cellulose, lignin, starch and chitin (Pu
103 et al., 2007; Silva et al., 2011; Wang et al., 2012; Wu et al., 2009). There are
104 several ILs that can directly dissolve cellulose upon heating, such as 1 -allyl-
105 3-methylimidazolium chloride (AMIM-Cl) and 1-ethyl-3-
106 methylimidazolium acetate (EMIM Ac) (Haward et al., 2012; Wu et al.,
107 2009). Furthermore, in recent years there has been a great interest of the
108 international scientific community on ILs, used as pharmaceutical
109 ingredients that can modify the pharmacokinetics and pharmacodynamics of
110 drugs (Moniruzzaman et al., 2010; Stoimenovski et al., 2010).

111 In biomedical applications and tissue engineering, there is need for soft
112 polymers which show more compatibility with the soft tissue as compared to
113 the stiff ones (Foster, 2017). While taking this into account, cellulose is not
114 only biocompatible and green, but also has advance applications while

115 working under biological conditions (Norhidayu Zainuddin, 2017a;
116 Rramaswamy Ravikumar, 2017).

117 In view of its bio-applications, and to reap the benefits of a pharmacological
118 drug, we have incorporated curcumin at different percentage by weight in a
119 matrix of cellulose dissolved by ionic liquid to manufacture curcumin
120 incorporated fibers. The focus of current work is to develop a simple but
121 effective manufacturing method which will allow continuous manufacturing
122 of strong cellulose/curcumin fibres. The strong cellulose/curcumin fibres
123 thus obtained has the potential to be woven into bandages and to use in drug,
124 food and cosmetic industry for various low cost affordable health care.

125

126 **2 Materials and Methods**

127 Cellulose pulp sheets (A4 size cardboard sheets) with a degree of
128 polymerization of 890 DP were purchased from Rayonier (Jacksonville, US).
129 Curcumin in powder, purity about 95%, was purchased from
130 <https://supplementsyou.com/> (Jersey, United Kingdom). The ionic liquid 1-
131 ethyl -3-methylimidazolium diethyl phosphate (emim DEP, >95%) was
132 obtained from Iolitec, and used without further purification.

133 **2.1 Cellulose/curcumin fibers formation**

134 The cellulose pulp sheets were finely chopped into (1×1 cm²) small pieces
135 using scissors and grinded into filaments using a Bosch MMB43G3BGB
136 Glass Jug Blender. To prepare cellulose/ curcumin composite fibers, 4 % of

137 cellulose (with respect to the mass of the ionic liquid) was dissolved in emim
138 DEP. The solution preparation was carried out in a fume hood using a
139 magnetic stirrer hotplate from Fisher Scientific (Loughborough, UK) with an
140 oil bath heated at 80 °C. The viscous solution was stirred for 6 h until there
141 was a complete dissolution of cellulose.
142 When the cellulose was dissolved 0 wt%, 1 wt%, 5 wt% and 10 wt% of
143 curcumin (with respect to the mass of cellulose) was added to the 4 wt%
144 cellulose/emim DEP solutions. The cellulose/emim DEP with 0 wt%, 1 wt%,
145 5 wt% and 10 wt% of curcumin was transferred into a 20-ml Luer lock
146 syringe (Terumo, UK). The solution in the syringe was degassed in a
147 vacuum oven at 60 °C overnight to remove any bubbles before spinning. A
148 lab-built spinning facility, which consists of a syringe pump, a deionized
149 water bath and a winding drum with a monitor, was used for the dry-jet wet
150 fiber spinning of cellulose (Figure 1). The cellulose/curcumin/emim DEP
151 solution was injected into the water bath at a fixed extrusion velocity ($V_1 =$
152 2.9×10^{-2} m/s), while the winding drum and electric motor were
153 continuously winding the fibers at varying winding velocities (V_2) of $1.5 \times$
154 10^{-1} m/s, 2.9×10^{-1} m/s and 4.8×10^{-1} m/s downstream. After spinning, the
155 fibers were immersed in deionized water for 2 days, with a change of water
156 every 24 h, and then rolled and dried in a fume hood for a further 48 h.
157 According to (Haward et al., 2012), the fibres spun under high extension rate
158 within the air gap tends to align better and shows high crystallinity.

159 Following the similar trend, here we have investigated the fibers spun with
160 the higher draw ratio.

161 In the fiber spinning process, the air gap between the die and the roller was
162 maintained at $d = 3\text{cm}$. Here, the draw ratio, $DR = V_2/V_1$ is the degree of
163 stretching applied to the fluid filament within the air gap. Here, V_1 is the
164 average velocity at which fluid is ejected from the die. V_2 is the velocity at
165 which fiber is taken up on the spool. $V_1 = Q/\pi r^2$, where Q is the volume flow
166 rate and r is the die radius. (Haward et al., 2012).

167 **2.3 Characterization techniques**

168 **2.3.1 Scanning electron microscopy**

169 Scanning electron microscopy (SEM) was used to study the morphology of
170 the fibres obtained and to measure the diameters of the fibres. The samples
171 (1 cm^2) were vacuum-coated with 10 nm thick layer of gold using an EMS
172 7620 Mini Sputter Coater/Glow Discharge System and were observed with
173 Jeol JSM-5510 (Jeol Ltd., Japan). For each kind of cellulose/curcumin fibre,
174 five different samples were analyzed with gold coating, and for each sample
175 three images at different locations were acquired using a TM3030 Plus
176 Tabletop scanning electron microscope from HITACHI (Berkshire, UK).
177 The mean diameter of the fibres was measured using the ImageJ software
178 package and standard deviation (SD) of each fibre samples were calculated
179 based on results from fifteen measurements which is supported by the
180 supplementary document where the true cross-sectional images for each type

181 of fibres was observed under microscope to conform the circular
182 approximately cross-section.

183 **2.3.2 Mechanical properties**

184 Tensile testing of the fibres was performed on a Dia-Stron Ltd. (Andover,
185 UK) at 25 °C, using 20N load cell under a constant deformation rate of 2
186 mm/min. To perform the tests, a gauge length of 2 cm was used. Ten
187 samples for each concentration of fibre (cellulose, 1% curcumin, 5%
188 curcumin and 10% curcumin) were analyzed. The fibres were glued to the
189 holding tabs to reduce the influence of clamping. Stress–strain curves were
190 obtained considering the cross-sectional area of the fibers as measured by
191 SEM. The ultimate tensile strength and strain were determined at the fibre
192 breaking point. The Young's modulus was calculated from the slope of the
193 linear portion of the stress–strain curve before the yield point.

194 **2.3.3 FTIR spectroscopy**

195 Fourier transform infrared spectroscopy was performed on a PerkinElmer
196 Spectrum 100 instrument and was used to identify the chemical bonds
197 between curcumin and cellulose and to investigate the presence of residue
198 emim DEP in the fibers after the water wash for 48 h. Four cumulative scans
199 with a resolution of 4 cm⁻¹ were taken in the wavenumber range from 4000
200 cm⁻¹ to 600 cm⁻¹ in transmittance mode.

201 **2.3.4 Wide Angle X-ray Diffraction**

202 The SAXSLAB GANESHA 300 XL SAXS system in the school of Physics
 203 at University of Bristol was used to study the structural pattern of the fibers
 204 in this study. Fibres spun at various velocity were mounted straight on the
 205 sample holder placed on a sample stage between the X-ray and the two-
 206 dimensional detector. Each fibre was exposed for around 4 hours to the Cu
 207 $K\alpha$ radiation with a wavelength of 0.154 nm in vacuum chamber to obtain
 208 the Wide-Angle X-ray Diffraction patterns for single fibre filaments. The
 209 sample-to-detector distance used was 100 mm, the beam size was 0.8 mm
 210 and the beam stop was 2 mm. IDL and SAXSGUI software are used for data
 211 reduction and analysis purposes.

212 Based on the XRD images, the orientation was calculated. In order to
 213 characterize the cellulose crystallite orientation in the fibers, the orientation
 214 factor ‘f’ is determined from the scattering data for each fiber as;

$$f = \langle P_2(\cos\theta) \rangle = \frac{(3\langle \cos^2\theta \rangle - 1)}{2} = (-2) \frac{\int_0^\pi \rho(\theta) P_2(\cos\theta) \sin\theta d\theta}{\int_0^\pi \rho(\theta) \sin\theta d\theta}$$

215
 216 Here, P_2 is the second order Legendre function. $\langle \cos^2\theta \rangle$ is the average polar
 217 disorientation angle of a crystallite w.r.t the fiber axis. θ is the azimuthal
 218 angle of the scattering in the diffraction pattern. $f = -0.5$ and $f = 1$, indicates
 219 the perfect orientation of cellulose crystallites would have in the
 220 perpendicular and a perfect orientation parallel to fiber axis respectively.

221 By Segal's law (Norhidayu Zainuddin, 2017a; Sameer S. Rahatekar, 2009),
222 the following equation was used to calculate the crystallinity index of the
223 fibres:

$$224 \text{CrI (\%)} = [(I_{002} - I_{am}) / I_{002}] \times 100\%$$

225 Where, I_{002} = peak intensities of crystalline region. And I_{am} = Peak intensity
226 for the amorphous region.

227 **2.3.5 Statistical analysis**

228 All data obtained after measuring the fibre diameter was analysed using
229 Prism software version 7. Two-way ANOVA with Bonferroni post-tests was
230 carried out; p value less than 0.0001 were considered significant. Mechanical
231 testing was subjected to the same analysis.

232

233 **3 Results**

234 **Surface Morphology:** The surface morphology of dry cellulose/
235 curcumin fibers were investigated using the optical microscope. All the
236 fibres maintained their continuity without any visible cracks.

237 **3.1 Scanning electron microscopy**

238 SEM images shown in Figure 2.1 and Figure 2.2 show the morphological
239 observation to greater extent. No sign of large clumps of curcumin particles
240 or sign of fibre breakage was observed in the samples with increasing
241 concentration of curcumin. Figure 2.2 shows the variation in the diameter of
242 10wt% cellulose/curcumin composite fibres spun at three different winding

243 speeds ie 0.15 m/s, 0.29 m/s and 0.48 m/s. As seen from figure 2.2 the
244 diameter of the cellulose/curcumin fibre decreases with increase in the
245 winding speed. Similar trend in reduction in fibre diameter with increase in
246 winding speed was observed for other set of fibres with difference curcumin
247 concentration. Additional experiments were carried out to check if the cross
248 section of the fibres is circular. The true cross-section of the cellulose fibres
249 are shown in supplementary information figure S1. As seen from this Figure
250 S1 the cross section of the all the cellulose and cellulose curcumin fibres are
251 nearly circular. The average diameters of the fibres at three different winding
252 velocities (V_2) of 0.15 m/s, 0.29 m/s and 0.48 m/s and different
253 concentration of curcumin are shown in Figure 3. Figure 3 showed no
254 effect of increase of curcumin concentration on the fibre diameter in various
255 groups represented in clusters of increasing curcumin concentration.
256 However different winding showed significant decrease in fibre diameter in
257 similar groups in all concentrations of curcumin studied. Hence the average
258 diameter of the fibers decreases with the increase in the winding velocities
259 but had no effect on it with increasing curcumin concentration. (Figure 3).

260 **3.2 Mechanical properties**

261 The fibres spun with maximum stable winding speed 0.48 m/s were used to
262 do the mechanical testing and further fibres characterization.

263 The tensile properties of the cellulose/curcumin fibres compared to the
264 values of the pure cellulose fibers has been shown in in Table 1.

265 As with tensile strength, the largest and the smallest values of the Young's
266 modulus were measured in 1% curcumin fibers (16.2 GPa) and 10%
267 curcumin fibers (13.06 GPa), respectively (Dai, 2016). However,
268 statistically no significant variation in the tensile strength was observed with
269 the increase of curcumin concentration.

270 **3.3 FTIR spectroscopy**

271 FTIR spectroscopy was used to confirm the presence of curcumin inside the
272 cellulose/curcumin fibers (Figure 4a and 4b). The peak at 1628 cm^{-1} present
273 in pure curcumin and the curcumin/cellulose fibers is from curcumin mixed
274 stretching vibrations of C=O and C=C bonds (Alfin Kurniawana, 2017)
275 (Mohanty and Sahoo, 2010). The peaks at 1429 cm^{-1} , found in pure curcumin
276 and cellulose/curcumin fibers are assigned to in plane bending of aromatic
277 (CCC, CCH) (Mohan et al., 2012; Pan et al., 2007).

278 Furthermore, The FTIR spectrum of the neat cellulose fibers (without
279 curcumin) was compared with those of as-received emim DEP (Figure S2,
280 supporting information) to find out if emim DEP is completely removed
281 from the regenerated fibres. In the FTIR spectrum of regenerated cellulose
282 and cellulose/curcumin fibers (Figure S2) the peaks associated with the
283 functional groups of solvent emim DEP, namely P=O (1250 cm^{-1})
284 (Bartholomew, 1972) (FitzPatrick et al., 2012) is not present which indicates
285 that the emim DEP solvent is completely removed from the regenerated
286 fibre.

287 **3.4 Wide Angle X-ray Diffraction (WAXD) of the Fibers**

288 Figure 5A shows the 2D diffraction pattern of cellulose and cellulose
289 curcumin composite fibres. The radial scanning data of cellulose (with
290 varying curcumin percentage) is shown in the Figure 5B. The intensity and
291 2-theta graph in Figure 5B clearly shows the diffraction pattern of the fibres
292 which is similar to that of the cellulose II crystal structure according to
293 previously reported work on cellulose fibres (Sameer S. Rahatekar, 2009).
294 The peak at two theta 12 degrees shows the 110 crystal plane, at 22 degrees
295 corresponds to 020 plane and at 28 degrees corresponds to the 002 crystal
296 plane in cellulose.

297 **3.5 Orientation Factor**

298 Figure 6 represents the effect of curcumin on cellulose fiber alignment which
299 is measured in terms of the orientation factor (refer to section 2.3.4). The
300 orientation factor of 1 represents complete alignment of polymer chains in
301 the direction of the fibre axis and the orientation factor 0 represents
302 completely random orientation of polymer chains in a given sample/fibre.
303 Figure 6 shows that with the increment in curcumin percentage from 0wt%
304 to 10wt%, the orientation factor of cellulose fibers decreases from 0.74 to a
305 lower value 0.69. Hence, the addition of curcumin partly disturbs the
306 orientation of cellulose chains in the fibers. Diagrammatic representation of
307 the same has been shown in Figure 6 in the boxes below the actual graph.

308 **3.6 Crystallinity Index**

309 The crystallinity of cellulose and cellulose curcumin fibers were calculated
310 using the Segal's equation as explained in section 2.3.4, the crystallinity
311 index of the fibres with curcumin concentration 0 wt%, 1 wt%, 5 wt% and
312 10 wt% was found to be 63%, 67%, 66% and 65% respectively.

313

314 **4. Discussion**

315 In this paper, we have successfully manufactured curcumin /cellulose based
316 fibres using ionic liquid as a solvent. The fibres have the potential to be used
317 in drug, cosmetic and food industry. Curcumin, a pharmacological product
318 which is obtained from a rhizome has been found to have anti-inflammation,
319 anti-oxidation and anti-cancer activities (Hualin Wang 2017; Jialing Pan,
320 2017; Qianyun Maa, 2017). In the past, various methods have to been used
321 to entrap curcumin to harness its medicinal benefits. Success has been
322 obtained in the form of membranes/ films(Qianyun Maa, 2017) fibrous
323 mats(Tsekova et al., 2017) nanoparticles(Sara Perteghella, 2017), nano
324 fibres (Norhidayu Zainuddin, 2017a, b) and electrospun fibres(Dai, 2016).
325 Due to its low solubility, alkaline nature and high degradation rate as well as
326 use of various synthetic carriers have however rendered its potential
327 unexplored.

328 On the other hand cellulose is widely used in drug (Norhidayu Zainuddin,
329 2017a; Rramaswamy Ravikumar, 2017), cosmetic and food packaging
330 industry (Nooshin Noshirvani, 2017; Prodyut Dhar, 2017). Here we have

331 manufactured curcumin based cellulose fibres in various concentrations and
332 at different winding speed. The fibres showed good dispersion of curcumin
333 as evident by the following set of experiments conducted, with SEM,
334 showing non-porous cross-sectional surface, FTIR- reflecting similar
335 curcumin peaks for all the tested samples and wide angle, X-ray diffraction
336 results confirming the consistency of results for each sample when compared
337 with the pure cellulose diffraction pattern.

338 Dispersion of curcumin in cellulose however renders its use in medical
339 science. Curcumin although has low solubility in water (Hongying Liang,
340 2017; Zeynep Aytac, 2017) but was found to be easily dispersed in ionic
341 liquid solution with cellulose. This entrapment of curcumin in fibre form
342 with cellulose which is highly biocompatible (Rramaswamy Ravikumar,
343 2017; Tsekova et al., 2017) thus renders it highly versatile in food packaging
344 industry.

345 The fibres thus obtained showed a decrease in the diameter with increase in
346 the winding speed (Figure 3). Similar results were obtained by Rahatekar (C.
347 Zhu1, 2013). This is due to the fact because in dry wet jet spinning, there is a
348 3 cm air gap between the spinneret and the water bath where the water get
349 stretched before entering in the coagulation process. This stretch helps in
350 better alignment of the fibre (Sameer S. Rahatekar, 2009). On increasing the
351 winding speed, the stretch in the fibre in the air gap as well as in the water

352 bath increases. This results in better alignment of the cellulose chains in the
353 fibre hence increasing the orientation parameter as shown in figure 6.

354 From SEM images, figure 2.1 and 2.2, no aggregated curcumin clumps were
355 found on the surface neither there was any evidence of breakage in fibre
356 surface due to aggregations.

357 From Table 1, the mechanical properties of our cellulose/curcumin
358 composite fibres showed no significant increase with the addition of more
359 curcumin to cellulose. According to Zainuddin (Norhidayu Zainuddin,
360 2017a), the addition of curcumin improves the mechanical properties of the
361 fibres moderately. But it starts decreasing with increase in curcumin
362 concentration due to the binding tendency of curcumin on the matrix surface,
363 which can be further improved by cross-linking process. Dai also observed
364 the improvement in the Young's modulus after adding the modified
365 curcumin particles in the fibre matrix, but there was no significant changes
366 when he analyzed the fibres dispersed with unmodified curcumin
367 particles(Dai, 2016). The tensile strength of the fibres obtained in our studies
368 were still higher than many viscose fibres being produced (Mouthuy, 2017);
369 (Alejandro Costoya, 2017; Marziyeh Ranjbar-Mohammadi, 2016; Shao-Zhi
370 Fu, 2014; Tsekova et al., 2017).

371 FTIR results corresponding from figure S2 also showed that the solvent peak
372 corresponding to emim DEP was not present in any of the regenerated
373 cellulose fibres which strongly indicated that the solvent emim DEP is

374 removed from the fibres. We also confirmed the presence of curcumin with
375 its characteristic peaks in cellulose/curcumin composites. Similar
376 characteristic peaks (Alfin Kurniawana, 2017) were observed by other
377 researchers in gelatin and curcumin composites (Dai, 2016) where they
378 manufactured electrospun curcumin gelatine blended nanofibrous mats and
379 water soluble complexes of curcumin with cyclodextrins (P.R. Krishna
380 Mohan, 2012).

381 The orientation factor of our fibres was found to be reduced with increase of
382 curcumin concentration as shown in figure 6. This is due to the limited
383 tendency of curcumin molecules to dissolve in the matrix. Up to certain
384 percentage curcumin supports the fibre crystal structure which has been
385 reported by (Dai, 2016), with further increase in concentration it acts as
386 impurity in the matrix and hinders the hydrogen bonding in the cellulose
387 matrix. This effect the alignment of the fibre as evident from results been
388 reported by (Norhidayu Zainuddin, 2017a), where Norhidayu found the
389 decrease in mechanical properties with increasing concentration of the
390 curcumin in the polymer matrix. Here when we relate the orientation factor
391 with mechanical properties of the fibres, it is clear that better aligned fibres
392 with good orientation factor shows improved mechanical properties and vice
393 versa (C. Zhu1, 2013; L.V. Haule, 2016).

394 X-ray analysis, corresponding to figure 5, however showed that addition of
395 curcumin (Marcela-Corina Roşu, 2017) in cellulose fibres doesn't have

396 significant difference on the degree of crystallization for all
397 cellulose/curcumin fibres compared with the neat cellulose fibres. These
398 values are similar to what earlier been reported by Rahatekar in (C. Zhu1,
399 2013; Sameer S. Rahatekar, 2009), where the cellulose fibres were spun
400 using wet spinning technique. As evident from Marcela's results where they
401 worked on the methylcellulose-based films containing graphenes and
402 curcumin (Marcela-Corina Roşu, 2017), it is clear that the curcumin has no
403 significant effect on the crystallinity index of the fibre matrix.

404 In this work, we have significantly improved the art of manufacturing
405 cellulose fibres reinforced with curcumin while working with different
406 concentration and winding speed. These fibres has the potential applications
407 in cosmetics, food industry, packaging and many other biomedical
408 applications as well.

409

410 **5. Conclusion**

411 In this report, we have manufactured strong regenerated cellulose and
412 cellulose/curcumin composite fibres (ranging from 1wt% to 10wt%
413 curcumin) with use of Emim DEP as a solvent. The increase in curcumin
414 concentration in cellulose fibres did not affect the fibre diameter. However
415 increased winding speed significantly reduced in the diameters of cellulose
416 and cellulose/curcumin composite fibres. Curcumin was found to be
417 uniformly dispersed in cellulose fibres as evident by SEM and optical

418 microscopy analysis. The tensile strength of regenerated cellulose/curcumin
419 fibres were found to be ranging from 223 to 336 MPa and Young's modulus
420 ranging from 13 to 14.9 GPa. The high winding speed resulted in efficient
421 alignment of cellulose chains as confirmed by X-ray diffraction, orientation
422 factor ranging from 0.69 to 0.74. However, increase in the curcumin
423 concentration caused small reduction in degree of alignment of cellulose
424 chains, no major change was observed in the crystallinity index of the fibres
425 due to addition of curcumin. In this work, we have successfully managed to
426 entrap curcumin in cellulose fibres which can have potential applications in
427 medical and food packaging industry.

428

429 **Acknowledgement:**

430 The authors would like to acknowledge the specialisation scholarship
431 funding from the Sapienza University Rome to support for Ms Marta Gina
432 Coscia. Ganesha X-ray scattering apparatus used for this work were
433 supported by an EPSRC Grant "Atoms to Applications" Grant ref
434 EP/K035746/1.

435

436 **Figure captions**

437 **Figure 1:** Schematic representation of the preparation of cellulose /curcumin
438 composite fibres.

439

440 **Figure 2.1:** Macroscopic and microscopic presentation of fibres. Cellulose
441 fibres with three varying concentration of curcumin were prepared namely:
442 0% (neat cellulose) A, A1; 1 % (cellulose with a concentration of 1%
443 curcumin, B, B1; 5 %(cellulose with a concentration of 5% curcumin), C,
444 C1; 10% (cellulose with a concentration 10% curcumin) D, D1; A, B, C, D
445 are macroscopic presentation of fibres with the scale bar showing 2 mm. A1,
446 B1, C1, D1 are the cross section of the fibres with SEM the scale bar shows
447 20 um.

448

449 **Figure 2.2:** SEM images for the Cellulose fibres with 10%curcumin
450 representing the decrease in diameter with increase in the winding speed
451 from 1.5×10^{-1} m/s, 2.9×10^{-1} m/s and 4.8×10^{-1} m/s.

452

453 **Figure 3:** Graphic representation of fibre diameter at different winding
454 velocities: 1.5×10^{-1} m/s, 2.9×10^{-1} m/s and 4.8×10^{-1} m/s. significant
455 statistical variation was seen in the fibre diameter with different winding
456 speed. Two-way ANOVA with Bonferroni post tests and a significance level
457 of 0.0001 was used. A mean \pm standard deviation format has been used to
458 present the data.

459

460 **Figure 4:** A) FTIR spectra of regenerated cellulose/curcumin fibres and
461 which show presence of curcumin peaks at 1429cm^{-1} and B) 1628cm^{-1} which

462 indicates that curcumin has retained its characteristic peaks though with less
463 intensity.

464

465 **Figure 5A:** WAXD image of (a) pure cellulose fibre (b) 10%
466 curcumin/cellulose fibre.

467

468 **Figure 5B:** Radial Scan of WAXD of (a) pure cellulose fibre (b) 10%
469 curcumin/cellulose fibre.

470

471 **Figure 6:** Variation in orientation factor in the orientation of the fibres while
472 processing in ionic liquid with the increase or curcumin.

473

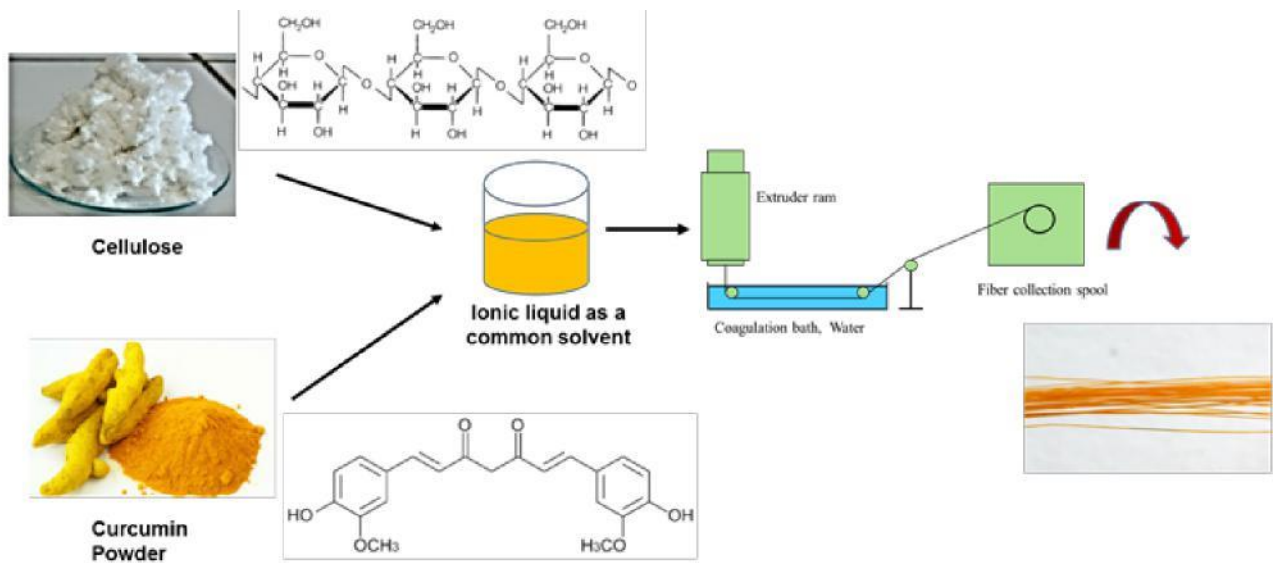
474 **Table 1:** Mechanical properties of cellulose/curcumin fibres and comparison
475 with pure cellulose fibres (0% curcumin).

476

477

478

479



480

481

Figure 1

482

483

484

485

486

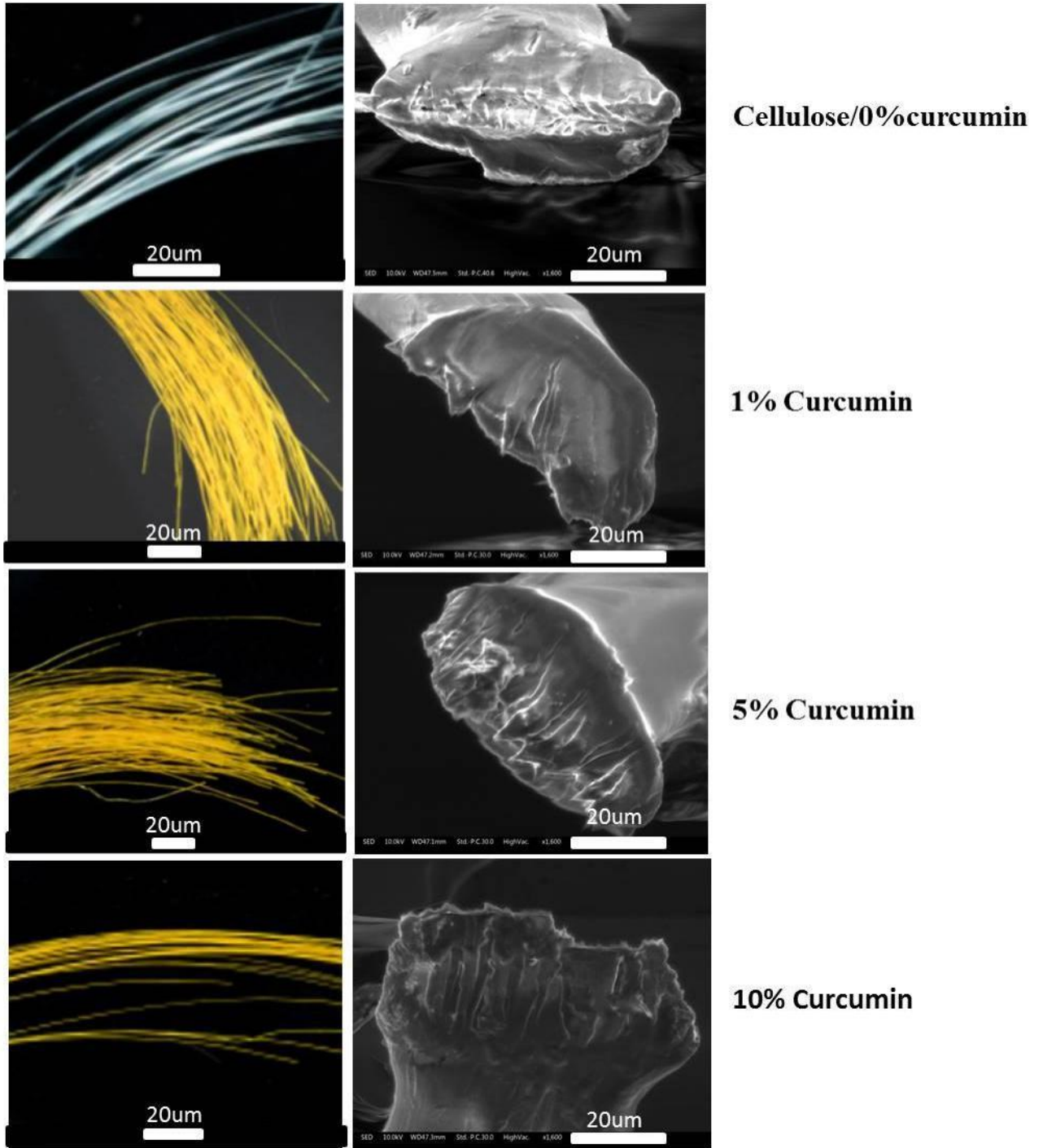


Figure 2.1

487

488

489

490

491

492
493
494
495
496
497
498
499
500
501
502
503
504
505
506
507
508

10% Curcumin Cellulose fibres

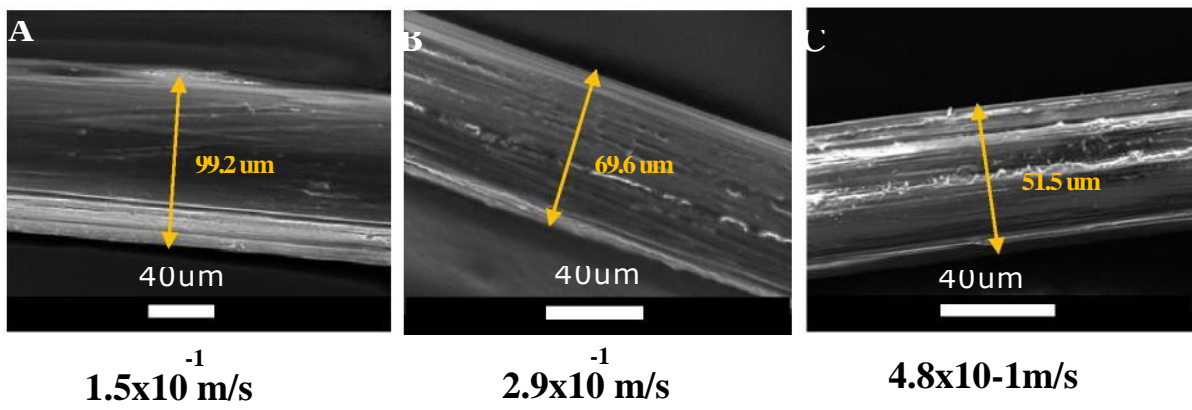


Figure 2.2

509

510

511

512

513

514

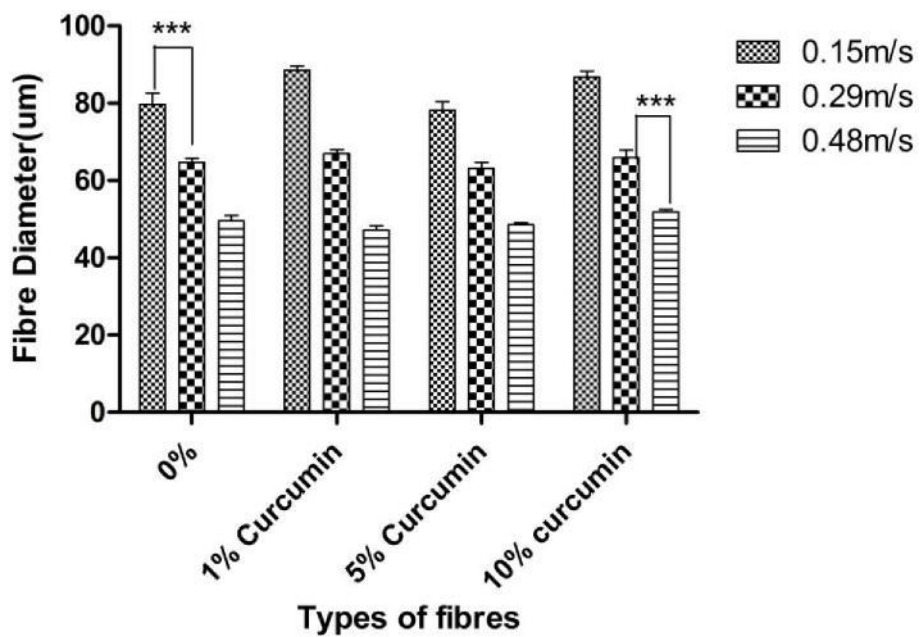
515

516

517

518

519



520

521

Figure 3

522

523

524

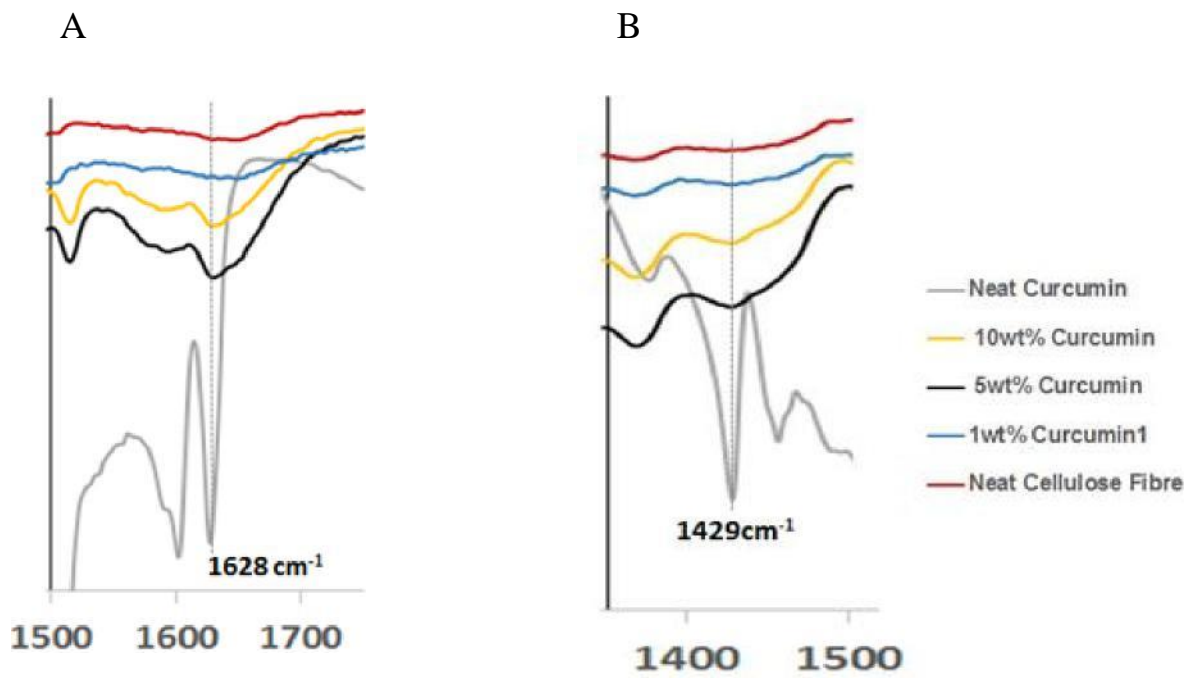
525

526

527

528

529



532

533

534

535

Figure 4

536

537

538

539

540

541

542

543

544

545

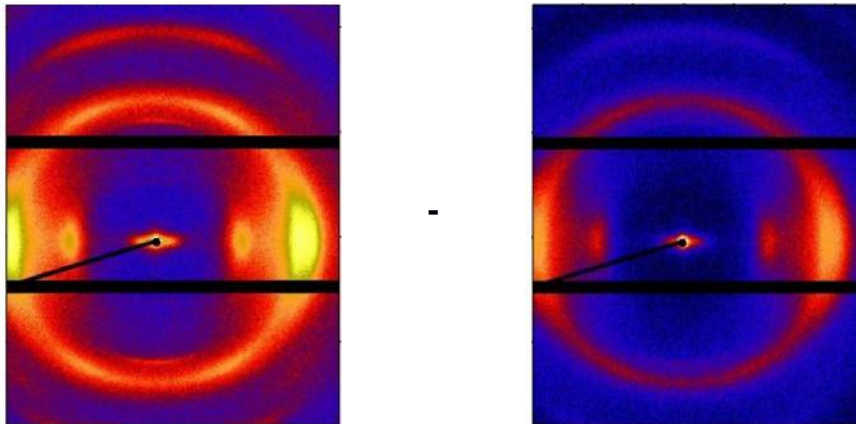
546

547

548

549

550



551

552

Figure 5A

553

554

555

556

557

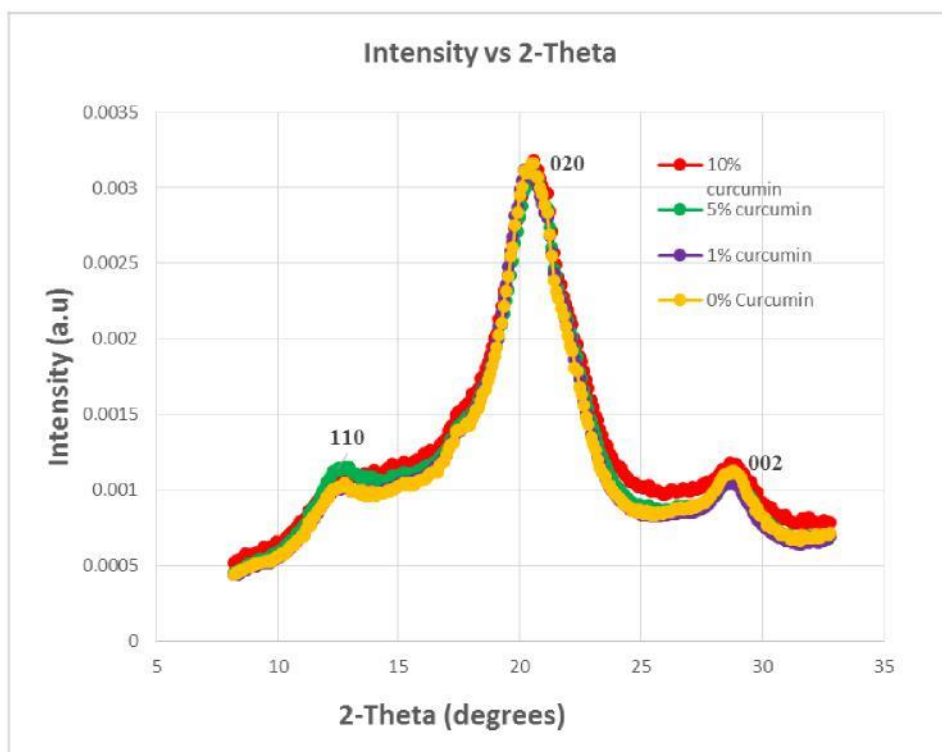
558

559

560

561

562



563

Figure 5B

564
565
566
567
568
569
570
571
572
573
574
575
576
577
578
579
580
581
582
583

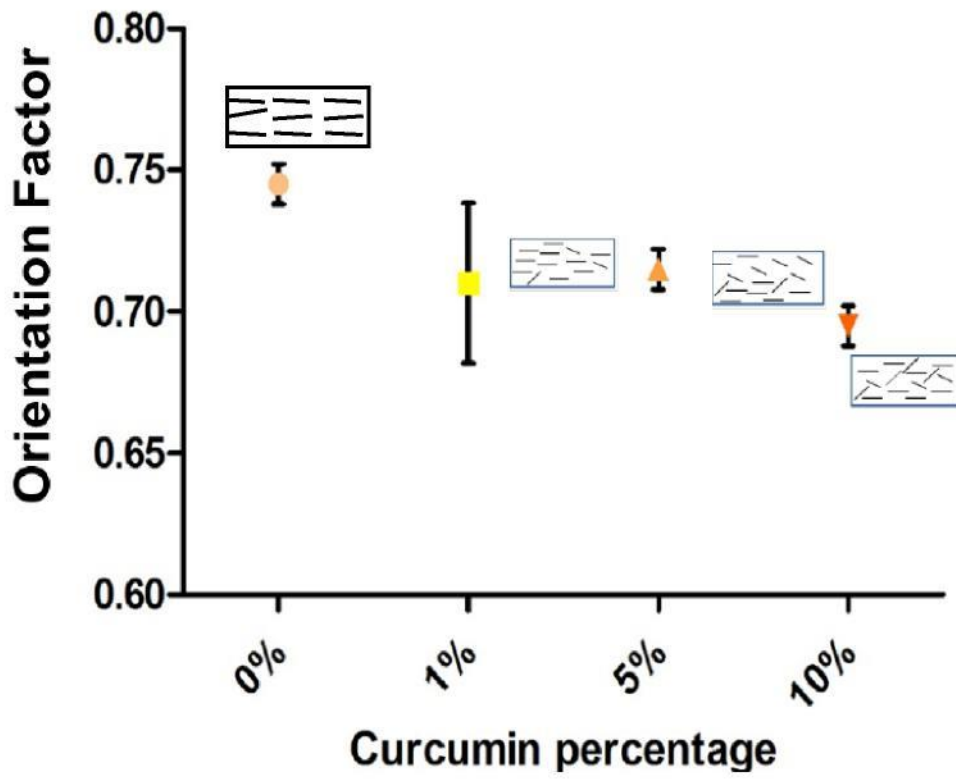


Figure 6

584
585
586
587
588
589
590
591
592
593
594
595
596
597
598
599
600
601
602
603

| Young's Modulus Sample GPa | Tensile Strength MPa | Strain % | Diameter of Fibre (μm) | |
|----------------------------------|--------------------------------|----------------------------------|---|--------------------------------|
| 0% Curcumin | 15.0\pm5.4 | 270.7\pm1.7 | 8.5\pm1.9 | 51.2\pm7.8 |
| 1% Curcumin | 16.2\pm1.6 | 336.7\pm4.4 | 11.2\pm3.8 | 46.3\pm4.1 |
| 5% Curcumin | 14.8\pm2.1 | 284.3\pm29.7 | 12.8\pm2.2 | 46.4\pm2.8 |
| 10% Curcumin | 13.6\pm2.1 | 223.2\pm22.1 | 9.9\pm1.8 | 51.7\pm.24 |

Table1

604 References:

- 605 Aggarwal, B.B., Kunnumakkara, A.B., Harikumar, K.B., Tharakan, S.T., Sung, B., Anand, P., 2008.
606 Potential of spice-derived phytochemicals for cancer prevention. *Planta medica* 74, 1560.
- 607 Alejandro Costoya, A.C.a.C.A.-L., 2017. Electrospun Fibers of Cyclodextrins and Poly(cyclodextrins).
608 *Molecules* 22.
- 609 Alfin Kurniawana, F.G., Adi Tama Nugrahaa, Suryadi Ismajib, Meng-Jiy Wang, 2017. Biocompatibility
610 and drug release behavior of curcumin conjugated gold nanoparticles from aminosilane-
611 functionalized electrospun poly (N-vinyl-2-pyrrolidone) fibers. *Int. J. Pharm.*
- 612 Bartholomew, R.F., 1972. Structure and properties of silver phosphate glasses - Infrared and visible
613 spectra. *Journal of Non-Crystalline Solids* 7, 221-235.
- 614 C. Zhu¹, J.C., K. K. Koziol², J. W. Gilman³, P. C. Trulove⁴, S. S. Rahatekar¹, 2013. Effect of fibre
615 spinning conditions on the electrical properties of cellulose and carbon nanotube composite fibres
616 spun using ionic liquid as a benign solvent. *Express Polym Lett* 8, 154-163.
- 617 Czaja, W.K., Young, D.J., Kawecki, M., Brown, R.M., 2007. The future prospects of microbial cellulose
618 in biomedical applications. *Biomacromolecules* 8, 1-12.
- 619 Dai, X., 2016. Electrospun curcumin gelatin blended nanofibrous mats accelerate wound healing by
620 Dkk-1 mediated fibroblast mobilization and MCP-1 mediated anti-inflammation.
- 621 de Moura, M.R., Mattoso, L.H.C., Zucolotto, V., 2012. Development of cellulose-based bactericidal
622 nanocomposites containing silver nanoparticles and their use as active food packaging. *Journal of*
623 *Food Engineering* 109, 520-524.
- 624 Eichhorn, S.J., Dufresne, A., Aranguren, M., Marcovich, N.E., Capadona, J.R., Rowan, S.J., Weder, C.,
625 Thielemans, W., Roman, M., Renneckar, S., Gindl, W., Veigel, S., Keckes, J., Yano, H., Abe, K., Nogi,
626 M., Nakagaito, A.N., Mangalam, A., Simonsen, J., Benight, A.S., Bismarck, A., Berglund, L.A., Peijs, T.,
627 2010. Review: current international research into cellulose nanofibres and nanocomposites. *J Mater*
628 *Sci* 45, 1-33.
- 629 FitzPatrick, M., Champagne, P., Cunningham, M.F., 2012. Quantitative determination of cellulose
630 dissolved in 1-ethyl-3-methylimidazolium acetate using partial least squares regression on FTIR
631 spectra. *Carbohydrate Polymers* 87, 1124-1130.
- 632 Foster, S. M.C.R.M.J.G.P.E.J., 2017. Mechanically switch able polymer fibers for sensing in biological
633 conditions. *J. Biomed. Opt* 22.
- 634 Granja, P., De Jeso, B., Bareille, R., Rouais, F., Baquey, C., Barbosa, M., 2005. Mineralization of
635 regenerated cellulose hydrogels induced by human bone marrow stromal cells. *Eur Cell Mater* 10,
636 31-37.
- 637 Granja, P.L., Barbosa, M.A., Pouysegue, L., De Jeso, B., Rouais, F., Baquey, C., 2001. Cellulose
638 phosphates as biomaterials. Mineralization of chemically modified regenerated cellulose hydrogels.
639 *J. Mater. Sci.* 36, 2163-2172.
- 640 Haward, S.J., Sharma, V., Butts, C.P., McKinley, G.H., Rahatekar, S.S., 2012. Shear and extensional
641 rheology of cellulose/ionic liquid solutions. *Biomacromolecules* 13, 1688-1699.
- 642 Holbrey, J., Rogers, R., 2002. Ionic liquids in synthesis. Wiley VCH Verlag GmbH and Co. KGaA.
- 643 Hongying Liang, J.M.F., Parimala Nacharaju, 2017. Fabrication of biodegradable PEG-PLA
644 nanospheres for solubility, stabilization, and delivery of curcumin. *Artif Cells Nanomed Biotechnol.*
645 45.
- 646 Hualin Wang, L.H., Peng Wang, Minmin Chen, Suwei Jiang, Shaotong Jiang, 2017. Release kinetics
647 and antibacterial activity of curcumin loaded zein fibers. *Food Hydrocoll.* 63, 437-446.
- 648 Ibrahim, H.S., Ammar, N.S., Soyak, M., Ibrahim, M., 2012. Removal of Cd(II) and Pb(II) from aqueous
649 solution using dried water hyacinth as a biosorbent. *Spectrochimica Acta Part A: Molecular and*
650 *Biomolecular Spectroscopy* 96, 413-420.
- 651 Imran, M., El-Fahmy, S., Revol-Junelles, A.M., Desobry, S., 2010. Cellulose derivative based active
652 coatings: Effects of nisin and plasticizer on physico-chemical and antimicrobial properties of
653 hydroxypropyl methylcellulose films. *Carbohydr. Polym.* 81, 219-225.

654 Jialing Pan, T.X., Fengli Xu, Yali Zhang, Zhiguo Liu, Wenbo Chen, Weitao Fu, Yuanrong Dai, Yunjie
655 Zhao, Jianpeng Feng, Guang Liang, 2017. Development of resveratrol-curcumin hybrids as potential
656 therapeutic agents for inflammatory lung diseases. *Eur. J. Med. Chem.* 125.
657 Kaefer, C.M., Milner, J.A., 2008. The role of herbs and spices in cancer prevention. *The Journal of*
658 *Nutritional Biochemistry* 19, 347-361.
659 Kontturi, E., Tammelin, T., Österberg, M., 2006. Cellulose—model films and the fundamental
660 approach. *Chemical Society Reviews* 35, 1287-1304.
661 Mahmood, K., Zia, K.M., Zuber, M., Salman, M., Anjum, M.N., 2015. Recent developments in
662 curcumin and curcumin based polymeric materials for biomedical applications: A review.
663 *International journal of biological macromolecules* 81, 877-890.
664 Marcela- Corina oşu , . . , Crina ocaci, L idia M5 geruş an, Iorina og5 cean, Maria Coroş, A lex andru
665 Turza, Stela Pruneanu, 2017. Cytotoxicity of methylcellulose-based films containing graphenes and
666 curcumin on human lung fibroblasts. *Process Biochem.* 52.
667 Martson, M., Viljanto, J., Hurme, T., Laippala, P., Saukko, P., 1999. Is cellulose sponge degradable or
668 stable as implantation material? An in vivo subcutaneous study in the rat. *Biomaterials* 20, 1989-
669 1995.
670 Marziyeh Ranjbar-Mohammadi, S.R., S. Hajir Bahrami, M.T. Joghataei, F. Moayer, 2016. Antibacterial
671 performance and in vivo diabetic wound healing o cu rcu min loaded gum tragacanth/ pol (ε-
672 caprolactone) electrospun nanofibers. *Mater Sci Eng C Mater Biol Appl* 69.
673 Miyamoto, T., Takahashi, S.i., Ito, H., Inagaki, H., Noishiki, Y., 1989. Tissue biocompatibility of
674 cellulose and its derivatives. *Journal of biomedical materials research* 23, 125-133.
675 Mohan, P.K., Sreelakshmi, G., Muraleedharan, C., Joseph, R., 2012. Water soluble complexes of
676 curcumin with cyclodextrins: Characterization by FT-Raman spectroscopy. *Vibrational Spectroscopy*
677 62, 77-84.
678 Mohanty, C., Sahoo, S.K., 2010. The in vitro stability and in vivo pharmacokinetics of curcumin
679 prepared as an aqueous nanoparticulate formulation. *Biomaterials* 31, 6597-6611.
680 Moniruzzaman, M., Tahara, Y., Tamura, M., Kamiya, N., Goto, M., 2010. Ionic liquid-assisted
681 transdermal delivery of sparingly soluble drugs. *Chem Commun* 46, 1452-1454.
682 Mouthuy, P.-A . . Š . , Maj a; Č ipak aš parov ić, Ana; Milk ov ić, L idij a; Carr, Andrew, . h sico-
683 chemical and biological characterisation of the use of curcumin-loaded electrospun filaments for soft
684 tissue repair applications. *FULIR*.
685 Müller, F.A., Müller, L., Hofmann, I., Greil, P., Wenzel, M.M., Staudenmaier, R., 2006. Cellulose-based
686 scaffold materials for cartilage tissue engineering. *Biomaterials* 27, 3955-3963.
687 Nooshin Noshirvani, B.G., Reza Rezaei Mokarram, Mahdi Hashemi, Véronique Coma, 2017.
688 Preparation and characterization of active emulsified films based on chitosan-carboxymethyl
689 cellulose containing zinc oxide nano particles. *Int. J. Biol. Macromolec* 99.
690 Norhidayu Zainuddin, I.A., Hanieh Kargarzadeh, Suria Ramli, 2017a. Hydrophobic kenaf
691 nanocrystalline cellulose for the binding of curcumin. *Carbohydrate Polymers* 163, 261-269.
692 Norhidayu Zainuddin, I.A., Hanieh Kargarzadeh, Suria Ramli, 2017b. Hydrophobic kenaf
693 nanocrystalline cellulose for the binding of curcumin. *Carbohydr Polym* 163.
694 P.R. Krishna Mohan, G.S., C.V. Muraleedharan, Roy Joseph, 2012. Water soluble complexes of
695 curcumin with cyclodextrins: Characterization by FT-Raman spectroscopy. *Vib Spectrosc.*
696 Pan, C., Tang, J., Shao, Z., Wang, J., Huang, N., 2007. Improved blood compatibility of rapamycin-
697 eluting stent by incorporating curcumin. *Colloids and surfaces B: Biointerfaces* 59, 105-111.
698 Poustis, J., Baquey, C., Chauveaux, D., 1994. Mechanical properties of cellulose in orthopaedic
699 devices and related environments. *Clinical Materials* 16, 119-124.
700 Prodyut Dhar, S.S.G., Narendren Soundararajan, Arvind Gupta, Siddharth Mohan Bhasney, Medha
701 Milli, Amit Kumar, and Vimal Katiyar, 2017. Reactive Extrusion of Polylactic Acid/Cellulose
702 Nanocrystal Films for Food Packaging Applications: Influence of Filler Type on Thermomechanical,
703 Rheological, and Barrier Properties. *Ind. Eng. Chem. Res.* 56.

704 Pu, Y., Jiang, N., Ragauskas, A.J., 2007. Ionic liquid as a green solvent for lignin. *Journal of Wood*
705 *Chemistry and Technology* 27, 23-33.

706 Qianyun Maa, Y.R., Lijuan Wang, 2017. Investigation of antioxidant activity and release kinetics of
707 curcumin from tara gum/ polyvinyl alcohol active film. *Food Hydrocoll.* 70.

708 Ramsewak, R.S., DeWitt, D.L., Nair, M.G., 2000. Cytotoxicity, antioxidant and anti-inflammatory
709 activities of Curcumins I-III from *Curcuma longa*. *Phytomedicine* 7, 303-308.

710 Ramaswamy Ravikumar, M.G., Udumansha Ubaidulla, Eun Young Choi, Hyun Tae Jang, 2017.
711 Preparation, characterization, and in vitro diffusion study of nonwoven electrospun nanofiber of
712 curcumin-loaded cellulose acetate phthalate polymer. *Saudi Pharm J.*

713 Ruby, A.J., Kuttan, G., Dinesh Babu, K., Rajasekharan, K.N., Kuttan, R., 1995. Anti-tumour and
714 antioxidant activity of natural curcuminoids. *Cancer Letters* 94, 79-83.

715 Sameer S. Rahatekar, A.R., Rahul Jain, Mauro Zammarano, Krzysztof K. Koziol, Alan H. Windle, Jeffrey
716 W. Gilman, Satish Kumar, 2009. Solution spinning of cellulose carbon nanotube composites using
717 room temperature ionic liquids. *Polym. J* 50.

718 Sara Perteghella, B.C., Laura Catenacci, Milena Sorrenti, Giovanna Brunib, Vittorio Necchi, Barbara
719 Vigani, Marzio Sorlini, Maria Luisa Torre, Theodora Chlapanidas, 2017. Stem cell-extracellular
720 vesicles as drug delivery systems: New frontiers for silk/curcumin nanoparticles. *Int. J. Pharm.*

721 Shao-Zhi Fu, X.-H.M., Juan Fan, Ling-Lin Yang, Qing-Lian Wen, Su-Juan Ye, Sheng Lin, Bi-Qiong Wang,
722 Lan-Lan Chen, Jing-Bo Wu, Yue Chen, Jun-Ming Fan, Zhi Li, 2014. Acceleration of dermal wound
723 healing by using electrospun curcumin- (ε-caprolactone)-poly(ethylene glycol)- (ε-
724 caprolactone) fibrous mats. *J Biomed Mater Res B Appl Biomater* 102.

725 Sidhu, G.S., Mani, H., Gaddipati, J.P., Singh, A.K., Seth, P., Banaudha, K.K., Patnaik, G.K., Maheshwari,
726 R.K., 1999. Curcumin enhances wound healing in streptozotocin induced diabetic rats and genetically
727 diabetic mice. *Wound Repair and Regeneration* 7, 362-374.

728 Sidhu, G.S., Singh, A.K., Thaloor, D., Banaudha, K.K., Patnaik, G.K., Srimal, R.C., Maheshwari, R.K.,
729 1998. Enhancement of wound healing by curcumin in animals. *Wound Repair and Regeneration* 6,
730 167-177.

731 Silva, S.S., Duarte, A.R.C., Carvalho, A.P., Mano, J.F., Reis, R.L., 2011. Green processing of porous
732 chitin structures for biomedical applications combining ionic liquids and supercritical fluid
733 technology. *Acta biomaterialia* 7, 1166-1172.

734 Sonkaew, P., Sane, A., Suppakul, P., 2012. Antioxidant activities of curcumin and ascorbyl dipalmitate
735 nanoparticles and their activities after incorporation into cellulose-based packaging films. *Journal of*
736 *agricultural and food chemistry* 60, 5388-5399.

737 Stoimenovski, J., MacFarlane, D.R., Bica, K., Rogers, R.D., 2010. Crystalline vs. Ionic Liquid Salt Forms
738 of Active Pharmaceutical Ingredients: A Position Paper. *Pharmaceutical Research* 27, 521-526.

739 Svensson, A., Nicklasson, E., Harrah, T., Panilaitis, B., Kaplan, D., Brittberg, M., Gatenholm, P., 2005.
740 Bacterial cellulose as a potential scaffold for tissue engineering of cartilage. *Biomaterials* 26, 419-
741 431.

742 Tsekova, P.B., Spasova, M.G., Manolova, N.E., Markova, N.D., Rashkov, I.B., 2017. Electrospun
743 curcumin-loaded cellulose acetate/polyvinylpyrrolidone fibrous materials with complex architecture
744 and antibacterial activity. *Mater Sci Eng C Mater Biol Appl* 73, 206-214.

745 Vimala, K., Yallapu, M.M., Varaprasad, K., Reddy, N.N., Ravindra, S., Naidu, N.S., Raju, K.M., 2011.
746 Fabrication of curcumin encapsulated chitosan-PVA silver nanocomposite films for improved
747 antimicrobial activity. *Journal of Biomaterials and Nanobiotechnology* 2, 55.

748 Wang, H., Gurau, G., Rogers, R.D., 2012. Ionic liquid processing of cellulose. *Chemical Society*
749 *Reviews* 41, 1519-1537.

750 Wu, R.-L., Wang, X.-L., Li, F., Li, H.-Z., Wang, Y.-Z., 2009. Green composite films prepared from
751 cellulose, starch and lignin in room-temperature ionic liquid. *Bioresource Technology* 100, 2569-
752 2574.

753 Yang, H., Yan, R., Chen, H., Lee, D.H., Zheng, C., 2007. Characteristics of hemicellulose, cellulose and
754 lignin pyrolysis. *Fuel* 86, 1781-1788.

755 Zeynep Aytac, T.U., 2017. Core-shell nanofibers of curcumin/cyclodextrin inclusion complex and
756 polylactic acid: Enhanced water solubility and slow release of curcumin. *Int. J. Pharm.* 518.

757

Cross-section Observation of Cellulose Fibres

To determine the true cross section of cellulose fibres, the cross-sections of regenerated cellulose-curcumin fibres were imaged using optical microscope. Six to seven randomly picked filaments of cellulose fibres with 0 %, 1 %, 5 % and 10 % curcumin were mounted vertically and parallel to each other into a cylindrical resin mold. A combination of PRIMETM 20LV epoxy resin and PRIMETM 20 slow hardener purchased from Gurit (Newport, UK) with a mix ratio (weight) of 100:26 was used for the moulds. After filament mounting, the moulds were cured at room temperature for 2 days. They were then polished perpendicular to the filament axis direction using a Buehler BetaTM grinder polisher and a VectorTM power head (Esslingen am Neckar, Germany).

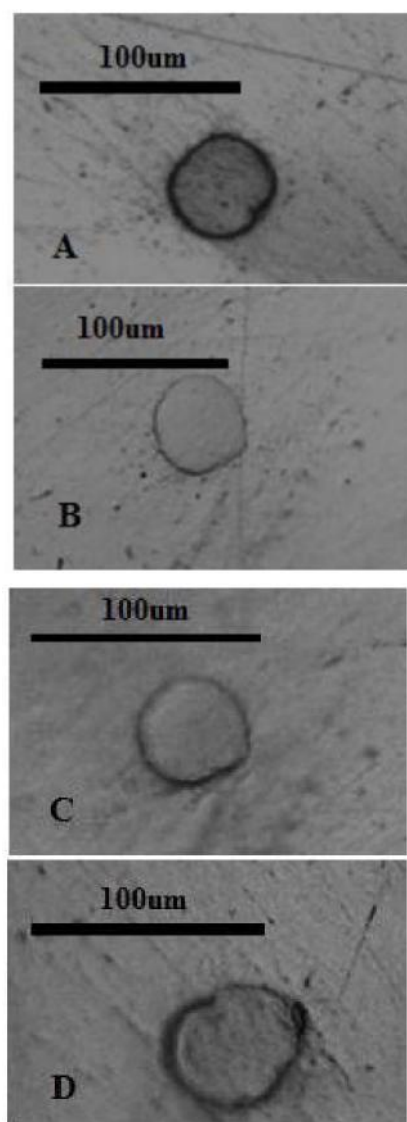


Figure S1. Microscopic image for cellulose fibres with (A) 0% curcumin fibres. (B) 1% curcumin fibres. (C) 5% curcumin fibres. (D) 10% curcumin fibres.

The cross-sectional shapes of fiber filaments mounted in resin moulds for cellulose fibers with 0 %, 1 %, 5 % and 10 % curcumin were observed using a ZEISS Axio Imager 2 microscope (Cambridge, UK).

It is clear from the cross-sectional images that the neat cellulose fibres and cellulose curcumin composite fibres (with 1wt %, 5wt % and 10wt % curcumin) has almost circular cross-section. Although there are impurities on the surface of the fibres that can be seen clearly from the figure 2.2, but doesn't have major contribution towards the diameter variations of the fibres. Following the work that has previously been done by our group (C. Zhu1, 2013), the diameter was measured from the fibre surface. Hence, it supports the calculated diameter values for the cellulose fibres with neat cellulose and cellulose/curcumin fibre composites (1 wt%, 5wt % and 10 wt% curcumin).

FTIR Spectroscopy for studying removal of emim DEP from cellulose fibres

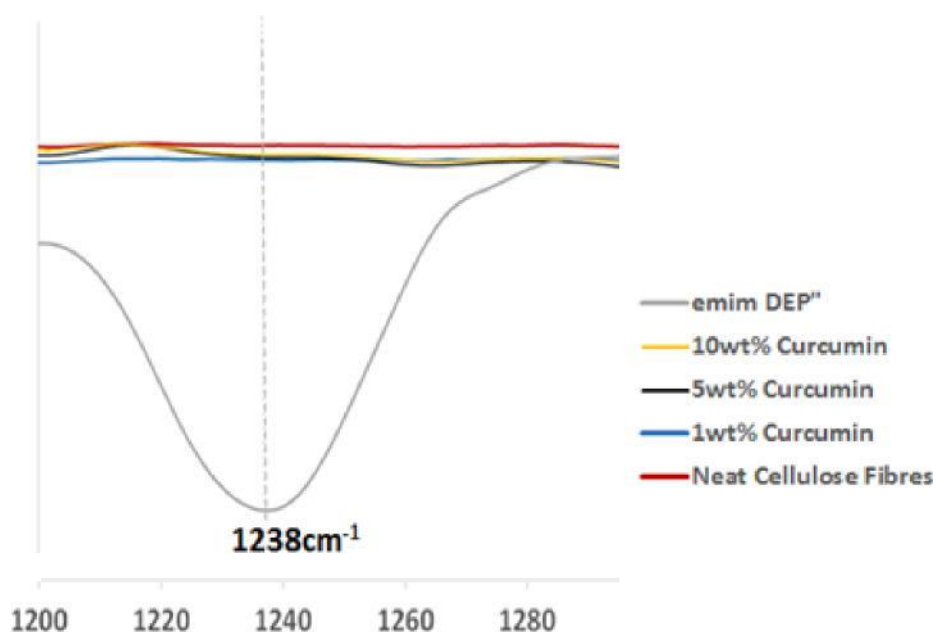


Figure S2. FTIR spectra of emim DEP solvent and the regenerated cellulose and cellulose/curcumin fibres; none of the regenerated cellulose fibres show the P=O bond peak at 1238cm^{-1} indicating that the solvent is completely removed from the fibres.

Reference:

C. Zhu, J.C., K. K. Koziol, J. W. Gilman, P. C. Trulove, S. S. Rahatekar, 2013. Effect of fibre spinning conditions on the electrical properties of cellulose and

carbon nanotube composite fibres spun using ionic liquid as a benign solvent.
Express Polym Lett 8, 154-163.

Manufacturing and characterization of regenerated cellulose/curcumin based sustainable composites fibers spun from environmentally benign solvents

Coscia, Marta Gina

2017-12-11

Attribution-NonCommercial-NoDerivatives 4.0 International

Coscia MG, Bhardwaj J, Singh N, et al., (2018) Manufacturing and characterization of regenerated cellulose/curcumin based sustainable composites fibers spun from environmentally benign solvents. *Industrial Crops and Products*, Volume 111, January 2018, pp. 536-543

<http://dx.doi.org/10.1016/j.indcrop.2017.09.041>

Downloaded from CERES Research Repository, Cranfield University